Article no. 2

THE CIVIL ENGINEERING JOURNAL 1-2020

FLEXURAL PERFORMANCE OF COLD-FORMED THIN-WALLED STEEL-PAPER STRAW BOARD COMPOSITE SLAB

Xiuhua Zhang, Zilin Zhao, Xiang Li

School of Civil Engineering, Northeast Forestry University, No. 26 Hexing Road, 150040 Harbin, China; 839714364@qq.com

ABSTRACT

A new type of composite slab was proposed by connecting paper straw board and cold-formed thin-walled steel with self-tapping screws. In order to investigate the failure process and failure mode of the composite slab, the tests on the flexural capacity of three composite slabs with different factors such as steel beam section size, beam spacing and the number of screws were carried out. The strain of the cold-formed thin-walled C-shaped steel and the paper straw board, and the deflection of the composite slab were observed, respectively. Moreover, the flexural behaviour and the composite action of the composite slab were investigated and the flexural capacity of the composite slab was obtained. It was found that the final failure mode of composite slab was the local buckling mode of cold-formed thin-walled C-shaped steel beam due to the adequate restraint of the straw board, and the reducing of the screw spacing had beneficial influence on the flexural yield capacity. The calculation method of midspan deflection and flexural capacity of composite slab were proposed, and the calculated values of deflection and flexural capacity agreed well with the test results. Therefore, the new composite slabs were of good working performance and high flexural capacity.

KEYWORDS

Composite slab, Paper straw board, Cold-formed thin-walled steel, Failure process, flexural behaviour

INTRODUCTION

Straw is a natural product of crops. At present, there is an oversupply of straw, which makes it cheap and easy to access in most countries. Because people are not aware of the cost and economic value of straw in many industries, it has not been widely used. The world's largest rice cultivators, such as India and China, suffer tremendously from the straw problems, because most of the current treatment methods are incineration on the spot. It not only wastes resources but pollutes the environment, and has a great impact on people's physical and mental health. Therefore, it is an urgent problem to make full use of the abundant straw resources for waste utilization. The employment of the renewable energy resource in buildings is greatly consistent with the concept of sustainable development, so paper straw board as a new environmentally protection building material emerges at the right moment [1-2].

Paper straw board (hereinafter called straw board) is a new environmentally friendly building material made from rice straw, which is directly heated and extruded in the molding machine to form a compact board, and glued on the surface with a layer of "protecting paper" of various materials. Straw board has many advantages as building materials. Firstly, straw board is more low-carbon and environmentally friendly than traditional building materials in terms of production and use. Secondly, it has good physical properties, including high strength, good seismic performance, excellent thermal insulation, good fire resistance and other characteristics.

Finally, it is cheap, which helps to reduce construction costs [3]. Studying lightweight composite members such as composite slabs and composite walls sheathed with straw boards can give full play to the respective advantages of different composite materials. It can not only use agricultural straw resources, reduce environmental pollution, but also conform to the new urbanization concept.

At present, compared with traditional reinforced concrete members, the lightweight composite member has the advantages of lightweight, economy and environmental protection for low-rise buildings constructed during urbanization. Slabs also play an important role as horizontal load bearing members in buildings. Up to now, many scholars had studied and applied various lightweight composite slabs [4-14] and achieved great results in stages. However, there were only a few reports on the composite action of straw board covering slab. In order to develop the type of lightweight composite slab, a new design of cold-formed thin-walled C-shaped steel-straw board composite slab was proposed. The failure process, failure mode and flexural capacity of composite slab were analyzed respectively through the experimental research on the flexural behaviour of specimens, and the deflection-load curves and load-strain curves of specimens were obtained, which provided basis for the theoretical analysis and engineering application of composite slab.

EXPERIMENT

Specimen details

According to reference [15] and *Technical Regulations for Low-rise Cold-formed Thin-walled Steel Buildings* (JGJ227-2011) [16], three composite slab specimens were tested for flexural capacity. The nominal short lip length and the nominal long lip length of specimens were 1200 and 2400mm, the span of support was 2200mm, and the straw board used for the specimen had a size of 2400mm×1200mm×58mm, respectively. The composite slabs were composed by the Q235B galvanized cold-formed thin-walled C-shaped steel and U-shaped track. The C-shaped steel beam and the U-shaped track were connected by ST3.5 self-tapping screw with a length of 16 mm, while the composite slab was connected by steel frame and straw board through ST4.8 self-propelled screws with a length of 75 mm, respectively. The self-tapping screw spacing was 150 and 300 mm in the periphery of the composite slab, and the screw spacing was 300 and 600 mm in the middle respectively. The four corners of the steel frame were respectively provided with shear connectors to ensure that possible local failures could not occur near the frame section of the support. The definitions of geometric parameters of specimen were illustrated in Figure 1 and specific parameters were listed in Table 1.

Tab. 1- Design parameters of specimens

Specimen no.	Slab size L×H/m	Beam type	Beam number	side beam type	Beam spacing /mm	Screw spacing /mm	
FL-1	2.4×1.2	C150×50×20×1.5	3	U153×50×1.5	600	150	300
FL-2	2.4×1.2	C150×50×20×1.5	3	U153×50×1.5	600	300	600
FL-3	2.4×1.2	C120×40×15×1.5	4	U123×40×1.5	400	150	300

DOI 10.14311/CEJ.2020.01.0002

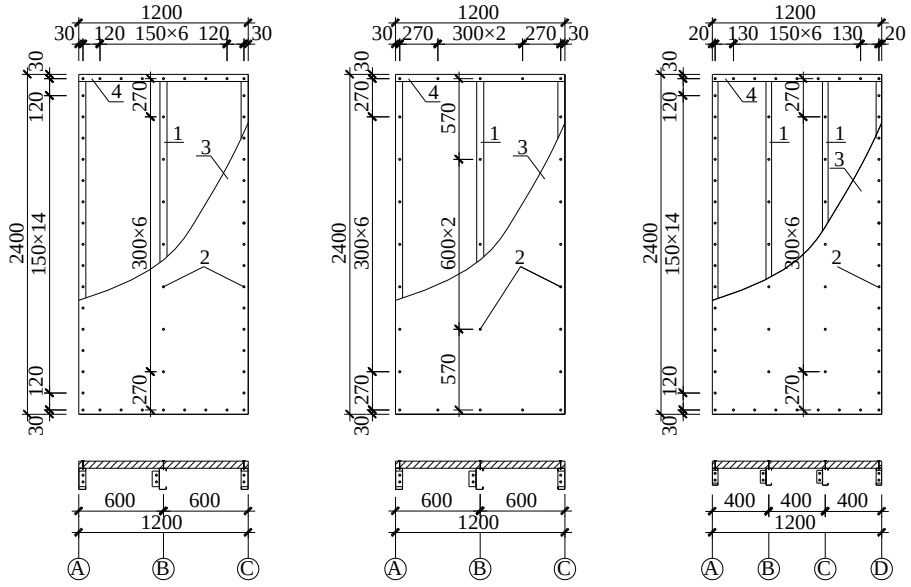

(a) – Specimen FL-1 *(b) – Specimen FL-2* *(c) – Specimen FL-3*

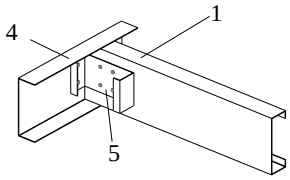

Note:
1- C-shaped steel beam
2- ST4.8 self-trapping screw
3- Paper straw board
4- U-shaped track
5- Shear connector
6- ST3.5 self-trapping screw

(d) – Shear connector

Fig. 1 – Construction and cross section of specimens

Material properties

The straw board material used in this test was provided by Harbin Tiancheng Shunjie Industrial Co., Ltd. The surface of rice straw board is flat, the thickness is 58mm, and the density is about 230-310kg/m^3. 75kg sand bag is used to impact the straw board at a height of 2m, the board is not damaged, and the impact resistance is good. The fire endurance is more than 1h, and the sound insulation of single side is up to 30dB.The steel frame was the Q235B galvanized cold-formed thin-walled steel produced by Angang with a thickness of 1.5mm. According to the *Tensile Test of Metal Material Part I: Room Temperature Test Method* (GB/T228.1-2010) [17], the steel was tested for metallic material properties as shown in Table 2.

Tab. 2- Mechanical properties of steel

Thickness /mm	Yield strength/MPa	Tensile strength/MPa	Elastic modulus/GPa	Elongation /%
1.5	274.3	372.7	198.3	31.97

The straw in the straw board was arranged in a herringbone shape and a kind of anisotropic materials. In accordance with the *Test Methods for Mechanical Properties of Wood-based Panels for Structures* (GB/T31264-2014) [18], the mechanical properties of paper straw board were listed in Table 3.

Tab. 3- Mechanical properties of paper straw board

Type	Rice straw direction	Flexural strength/MPa	Elastic modulus/MPa
Compression resistance	Parallel	0.67	358.5
	vertical	1.42	285.8
Flexural resistance	Parallel	1.87	400.6
	vertical	0.63	233.7

Test set-up and procedures

To simulate the uniform gravity loading of specimens，the test device applied for four-point bending test was shown in Figure 2. The specimen was simply supported with roller support on one side and pin support on the other side, and the fulcrum was 100mm away from the end of specimen, respectively. The specimen should be placed on the support along the length direction for adjustment and positioning. A 16t manual jack was used to apply the load through four spreader beams.

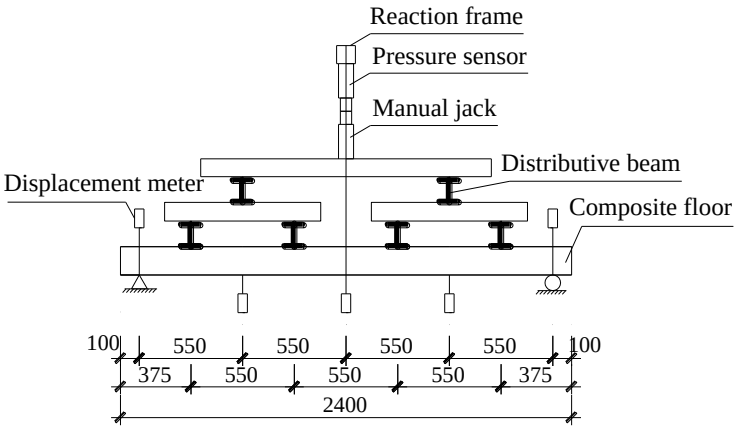

(a) – Test loading device

(b) – Test photo
Fig. 2 – Test set-up

The test loading system adopted the grading loading mode, which was carried out by the load control, and the load per stage did not exceed 10% of the estimated maximum load of each specimen. The preload was performed first before the official test, which preload was 5%~ 10% ultimate loads. After preloading, then unloaded, and then officially loaded. The load was kept for 1min after applying 4kN to each stage, and then data was collected. After the buckling of cold-

formed thin-walled C-shaped steel beam, the deformation of the specimen was observed and the relevant data and phenomena were recorded until the load reached the maximum value. When the load decreased to 80% of the peak load, it stopped loading.

Measuring-points arrangement

The test specimens were all symmetrical structures. In order to measure the variation of deflection and strain of specimens under flexural, the layout of the test points was shown in Figure 3. The displacement gauges labelled as D1-D8 were arranged to measure the deflection of specimen, and the strain gauges labelled as S1-S20 were arranged to measure the strain of specimen. In addition, five strain gauges were arranged on the upper and lower flanges and webs of each steel beam in the middle-spans, while three strain gauges were arranged on the upper and lower surfaces of straw board midspan section.

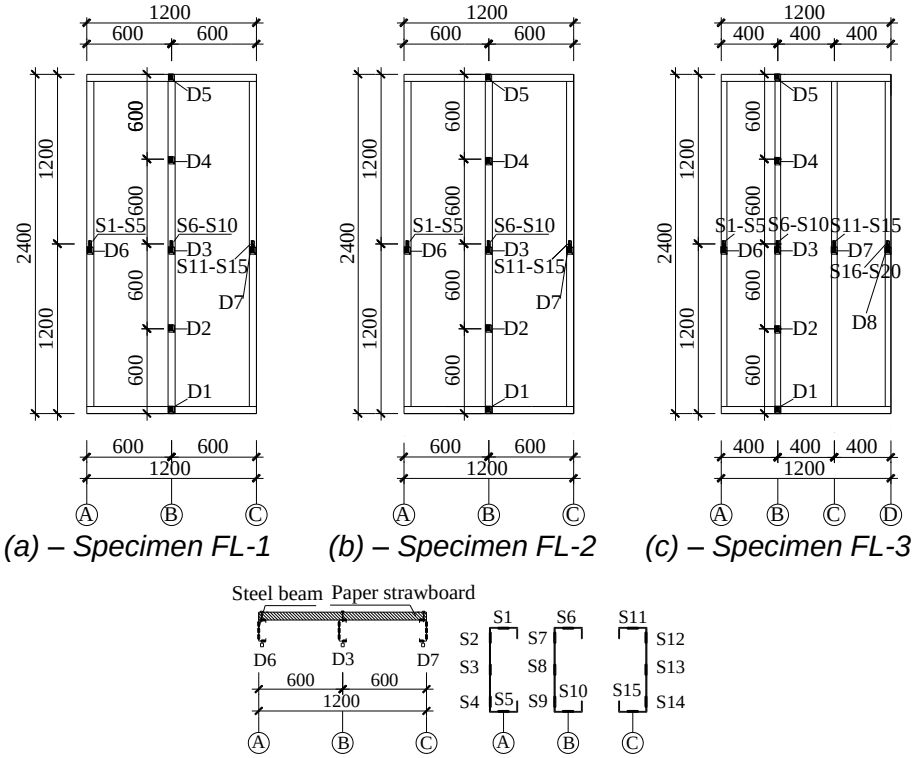

(a) – Specimen FL-1 *(b) – Specimen FL-2* *(c) – Specimen FL-3*

(d) – 1-1 Layout of measuring points

Fig. 3 – Measuring-point arrangement

THE TEST PHENOMENON

Test process and failure characteristics

(1) For specimens FL-1 and FL-2:

The stress process and failure phenomena of the test showed the basically same as that of specimen FL-1. Taking FL-1 as an example, the test process and failure characteristics were as follows. Firstly, the straw board and the steel frame were tightly connected and of good elasticity in the initial stage of the loading process, so deformations of the two were consistent. Both specimen FL-1 and FL-2 were in the elastic range, the wrinkles had appeared on the surface of the straw

board at the lower end of the spreader beam, and the steel and straw board were well coordinated. In addition, the specimen continued to emit a slight sound during the loading process. Then as the load increased, the wrinkles of the straw board gradually expanded outward, and the lower end of the spreader beam presented shallow concave wrinkles on the surface. The midspan deflection reached 12mm when the load reached about 40kN. Meanwhile, the straw board was deformed at the lower end of the spreader beam and the self-tapping screws near the middle of the specimen sank into the straw board (Figure 4(b)). There was severe torsion outside the plane to appear in the steel beams of specimen, which the outer steel beam-A was observed the largest rotation and obviously local buckling (Figure 4(c)), the middle steel beam-B was slightly torsional and local buckling (Figure 4(d)), the steel beam-C deformed slightly (Figure 4(e)), and the steel beams and straw board began to be separated. When the loading continued to 57.6kN, the pressure sensor reading decreased, there was a loud noise from the specimen suddenly, the steel beam-A was in lateral torsion and severe buckling failure occurred, and the failure degree of three beams decreased gradually from outside to inside, respectively. It was considered that the ultimate flexural capacity had been reached at this time. Lastly, the midspan deflection reached 20 mm at the end of the loading. Wrinkles on the straw board could be found, the bend of specimen could be observed obviously, and the steel frame was clearly separated from the straw board (Figure 4(f)). After unloading, removed the straw board and observed the failure of the steel frame (Figure 4(g)). The rest of the steel frame was basically intact except for the buckling failure of the side steel beam-A and the middle steel beam-B (Figure 4(h)), and the slight deformation of the steel beam-C, the upper and lower tracks and the supports.

(a) – Structural failure of specimen FL-1

(b) – Sinking of self-tapping screw

(c) – Local buckling of steel beam-A

(d) – Tendency of lateral torsion buckling of steel beam-B

Fig.4 – Failure modes of specimen FL-1

DOI 10.14311/CEJ.2020.01.0002

(e) – Deformation of steel beam-C

(f) – Separation of straw board and steel beam

(g) – Destruction of steel frame

(h) – Buckling failure details of steel beam-A and beam-B

Fig.4 – Failure modes of specimen FL-1

For the specimen FL-2, the increment was stable when the load is small, and there was no obvious deformation. Slight torsion occurred to the steel beams when loading to 38kN, both sinking of the self-tapping screw and separation of straw board and steel frame took place, and severe local buckling was observed on the outer steel beam-A and the middle steel beam-B webs at the same time. When the loading was continued to 55kN, the pressure sensor reading began to decrease and then was regarded as the specimen's ultimate bearing capacity of the load, buckling failure occurred to the outer steel beam-A (Fig. 5(b)), and the midspan deflection reached 26 mm.

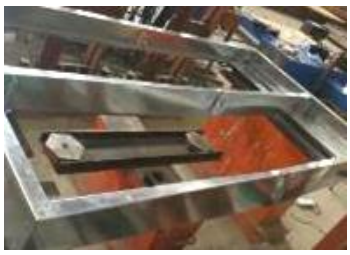

(a) – Destruction of steel frame

(b) – Local buckling of steel beam-A web

Fig.5 – Failure modes of specimen FL-2

(2) Specimen FL-3:

When the loading started, the load-deflection curve increased linearly and the deformation of the straw board and steel frame were consistent. The deformation continued to increase as the load increased to about 39kN, the specimen emitted a "squeak" sound in the loading process, and the straw board and the steel frame were slightly separated. Meanwhile, the midspan deflection reached 15mm. The load could not increase anymore when the load reached 56kN, that was to say, it reached its peak. Flexural buckling occurred to the outer steel beam-A (Figure 6(b)) and wrinkles on the straw board were observed respectively, while the midspan deflection reached 30mm.

(a) – Destruction of steel frame *(b) – Buckling failure of steel beam-A*

Fig.6 – Failure modes of specimen FL-3

ANALYSIS OF TEST RESULTS

Load-strain curve and analysis

The relationship curve between the load of test piece FL-3 and the strain of midspan section is shown in Figure7.

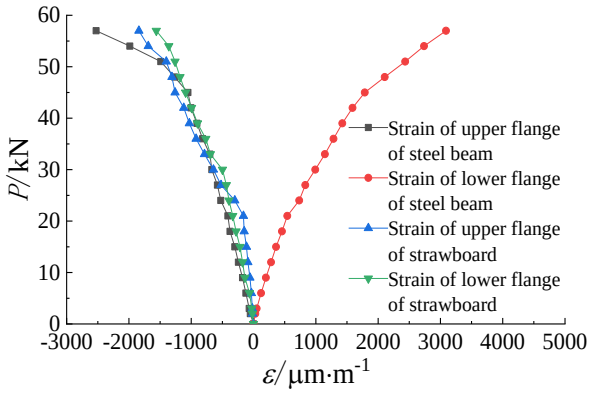

Fig.7 – Load-strain curves of midspan section

The upper flange of the C-shaped steel bears compressive stress while the lower flange bears tensile stress. Since the neutral axis of specimen is located above the symmetrical axis of the C-shaped steel due to composite action, the strain value of the tensioned side is larger than that of the compressed side.

In the initial stage of loading, the specimen is in the elastic stage and the load-strain curve grows linearly. The load-strain curve grows nonlinearly with the increase of load, and the specimen enters the elastoplastic stage. When the specimen approaches to the ultimate flexural capacity, the strain of the upper and lower flanges of the steel beam exceeds 2000$\mu\varepsilon$ indicating the steel beam exceeds the yield strength and the material properties of the steel beam are well applied. When the load is exerted, the strain values of upper and lower surface of the straw board are close to those of upper flange of the steel beam showing that the steel beam agrees well with the straw board and the overall working performance of the specimen formed by steel frame and the straw board is excellent. In addition, the strain values of the upper and lower surfaces of the straw board are negative indicating that the whole section of the straw board bears compressive stress during the whole loading process, which makes full use of the compressive performance of the straw board and avoids the shortcomings of poor tensile capacity of it. The load-strain curve of other specimens is similar to that of FL-3.

Figure 8 shows the distribution of the longitudinal strain along the height of the midspan section of the steel beam of the specimen. The abscissa represents the longitudinal strain of the section, the ordinate represents the height along the section, *y*=0mm expresses the edge of the lower flange of the steel beam, and *y*=150mm expresses the edge of the upper flange of the steel beam. It can be seen from Figure 7 and Figure 8 that the strain values of the upper and lower surface of the straw board are close to those of the upper flange of the steel beam. Therefore, the longitudinal strain distribution of the steel beams and the straw board basically conforms to the plane section assumption.

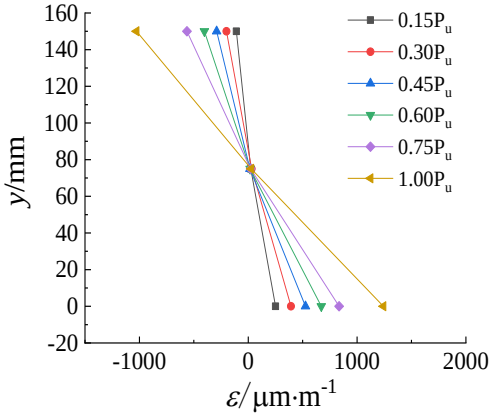

Fig.8 – Distribution of strain along the web of the midspan section of steel beam of specimen

Load-deflection curve and analysis

The load-deflection curves of three specimens are shown in Figure 9. The specimen is in the elastic stage at the initial stage of loading, the deflection of the specimen presents a linear growth, and the straw board and C-shaped steel show a good composite action. With the increase of load, the specimen enters the elastoplastic stage, the buckling of steel girder flange is caused by compression, the deflection of the midspan increases rapidly, and the flexural stiffness decreases. Continue loading, the buckling deformation of the specimen increased faster and the specimen is destroyed after reaching the ultimate flexural capacity. Continue loading after the load on the specimen reaches its ultimate flexural capacity, the load still decreases. Not stop loading until the load decreases to 80% of the ultimate flexural capacity.

Comparing the load-deflection curve of FL-1 and that of FL-2: the load-deflection curves of the two specimens almost coincide in the initial stage of loading and the screw spacing has no effect on the flexural capacity and flexural rigidity of the specimen. As the load increases, the specimen enters elastoplastic stage, the screws start to function, and the straw board restrains the steel frame to enter plastic stage. Increasing the screw spacing makes the lateral brace length of the specimen larger and the beam prone to local buckling. Therefore, the flexural rigidity of the specimen FL-2 with larger screw spacing decreases faster after buckling and the ultimate flexural capacity is smaller. Comparing the load-deflection curve of FL-1 to that of FL-3: the two load-deflection curves begin to separate after the initial loading stage, the flexural rigidity of FL-3 is smaller than that of FL-1, the ultimate flexural capacity of the two specimens are similar, but the flexural capacity of FL-3 decreases significantly faster after reaching the maximum load. The results indicate that the section size makes less influence on the stiffness of the member.

DOI 10.14311/CEJ.2020.01.0002

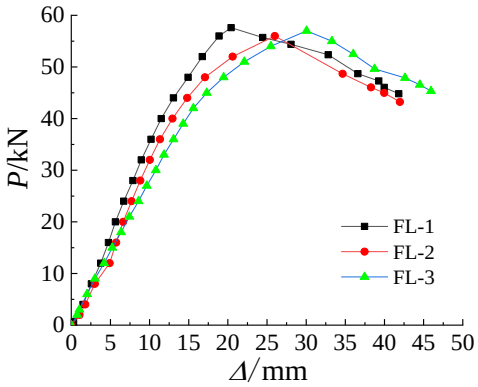

Fig.9 – Deflection-load curves

Flexural capacity characteristic value

The highest point on the load-deflection curve is the maximum load that the specimen can bear. After exceeding the load, the load-deflection curve enters the decreasing stage, the buckling failure appears to the steel beam, and then the load is continuously applied to cause the overall failure of the specimen. Because the flexural capacity of the specimen is mainly provided by the steel beam, so the corresponding load is defined as the yield load of the specimen when the steel beams of the specimen midspan begins to yield, that is, the load where the slope of the load-deflection curve suddenly changes is taken as the yield load of the specimen. The ultimate load and the ultimate displacement are the corresponding points when the load in the descending section is equal to 85% of the maximum load. According to the test results, yield load, ultimate load, midspan flexural displacement and the maximum displacements corresponding to ultimate load of three steel-straw board composite slabs are obtained as shown in Table 4.

Tab. 4 - Results of the test

Specimen No.	Yield load		Maximum load		Ultimate load	
	P_y/kN	Δ_y/mm	P_{max}/kN	Δ_{max}/mm	P_u/kN	Δ_u/mm
FL-1	39.92	11.39	57.60	20.42	48.96	37.29
FL-2	35.75	11.19	56.00	25.99	47.60	36.11
FL-3	36.92	13.45	57.00	30.04	48.45	40.63

According to the deflection limit requirements of flexural members in *Technical Specification for Low-rise Cold-formed Thin-walled Steel Buildings* (JGJ227-2011), the deflection limit of specimens is 11mm (L/200). When the specimens FL-1, FL-2, and FL-3 reach the serviceability limit state, the corresponding loads are 17.65kN/m^2, 16.05kN/m^2, and 14.02kN/m^2, respectively about 66.86%, 62.55% and 53.67% of their maximum loads. Therefore, it is important to improve the stiffness for member to meet the serviceability limit state. The test results show that the yield load of specimen FL-1 with smaller screw spacing is 11.66% higher than that of specimen FL-2 with larger screw spacing, indicating that the screw spacing effects the yield load of the specimen significantly.

Comparison results of tests

In order to make comparison of the test results more accurate, the composite slabs with the same section height are selected, and the flexural capacity of the composite slabs in other papers is converted into the unit width of flexural capacity. The test results of two specimens in this paper are compared with those of lightweight composite slab specimens in other papers as shown in Table 5.

Compared with different cover panels, the flexural capacity of cold-formed thin-walled C-shaped steel-straw board composite slab is about 41% higher than that of cold-formed thin-walled C-shaped steel-bamboo rubber composite slab. Compared with different steel types, the flexural capacity of cold-formed thin-walled C-shaped steel-straw board composite slab is increased by about 7.2% than that of profiled steel sheet-straw board composite slabs. Compared with different cover panels and steel types, the flexural capacity of cold-formed thin-walled C-shaped steel -straw board composite slab is about 12.4% higher than that of profiled steel sheet-straw board composite slabs. It can be seen from the results that the maximum displacement of cold-formed thin-walled C-shaped steel-straw board composite slab is larger, but its flexural displacement is smaller, indicating that its deformation capacity is better in the elastic stage. Obviously, the cold-formed thin-walled C-shaped steel-straw board composite slab exhibits the high flexural capacity.

Tab. 5 - Comparison of test results

Paper	Specimen No.	Steel yield Strength /MPa	Covering slab type	Steel type	Steel thickness /mm	Connection type	M_t /kN·m	Δ_{max} /mm
This paper	FL-1 FL-3	274.3	58mm thick straw board	cold-formed thin-walled C-shaped steel	1.5	self-propelled screw	11.01 10.03	20.42 30.04
paper5	B-3 B-4	265.5	double 5.2-11mm bamboo plywood	profiled steel sheet	0.7 0.7	sticky	6.84 8.07	22.51 16.10
paper9	B-1 B-2	334.04	double 9mm bamboo plywood	cold-formed thin-walled C-shaped steel	1.0	self-propelled screw, sticky, stainless steel rivet	10.01 9.61	23.74 24.19
paper12	S-1 S-4	235.0	one-sided 58mm thick straw board	profiled steel sheet	0.8 0.8	self-propelled screw	9.05 9.67	13.00 17.54

THE THEORY ANALYSIS

Calculation of deflection

It can be seen from the test results that the straw board and the steel beam are in the elastic stage under the serviceability limit state, the strain values of the two materials are basically similar, and the composite action is better. Therefore, it can be regarded as an integral elastic member for calculation when calculating the stiffness of composite slab.

According to the equation of material mechanics, the flexural stiffness of the composite slab is calculated according to Equations. (1):

$$EI_x = E_d I_d + E_s I_s \quad (1)$$

Where E_d is the elastic modulus of the straw board, Id is the moment of inertia of the straw board to the neutral axis, E_s is the elastic modulus of the steel beam, taking 1.983×105MPa, and I_s is the moment of inertia of the steel beam to the neutral axis.

The equation for calculating the midspan deflection of a simple support plate under uniform load is as follows:

$$\Delta = \frac{5ql^4}{384EI_x} \quad (2)$$

This test is a four-point load and the known deflection is calculated as:

$$\Delta = \frac{6.04Pl^3}{384EI_x} \quad (3)$$

Combining Eqs. (3) and (4), the uniform load of the composite slab is calculated as:

$$q = \frac{1.21P}{lb} \quad (4)$$

Where Δ is the midspan deflection of the composite slab, P is the load value of the composite slab obtained by the test, l is the distance between the two supports, E is the elastic modulus of the steel beam and is taking as 1.983×10^5MPa, I_x is the inertia moment of the composite slab and b is the width of the composite slab.

The loading mode used in the test is to simulate the uniform load at the four points. The experimental deflection value Δ_t and theoretical deflection value Δ_c are compared when the composite slabs achieve yield strength as shown in Table 6. The test deflection value is in good agreement with the theoretical deflection value in Table 6, and the error is controlled within 13%. Therefore, it is feasible to calculate the deflection using the Equations. (2) during the normal service stage of the composite slabs.

Tab. 6 - The deflection value of the composite slabs

Specimen No.	Δ_t/mm	Δ_c/mm	Δ_c/Δ_t
FL-1	11.39	11.04	0.97
FL-2	11.19	9.91	0.89
FL-3	13.45	13.47	1.01

Calculation of flexural capacity

The composite action associated with the straw board and steel frame demonstrates a better performance and the straw board and the steel beam can deform cooperatively according to the test results. Following the theory of sectional flexural capacity of composite structures, the failure section of composite slab is calculated as follows:

(1) When the flexural capacity of the specimen decreases to 85%, it is considered the failure of it while the upper and lower flanges of the steel beam yield currently.

DOI 10.14311/CEJ.2020.01.0002

(2) When the failure of specimen takes place, the strain of the straw board takes the yield strain of the steel beam, the whole section of the straw board bears pressed and it is always in the elastic stage.

According to the above conditions, the equations for calculating the flexural capacity of composite slabs are as follows, and the sectional form of the composite slab is shown in Figure 10.

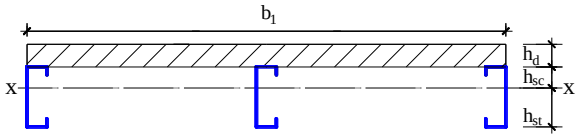

Fig.10 – Section form of composite slab

$$M = n\varphi f_{ys}(A_{sc}h_{sc} + A_{st}h_{st})/2 + \sigma_d A_d (h_{sc} + h_d/2) \quad (5)$$

Where n is the number of steel beams, f_{ys} is the buckling strength of the steel beam, φ is the integral stability coefficient of the steel beam and is taking as 0.9, h_{sc} is the distance from the resultant force center of the steel beam to the neutral axis, h_{st} is the distance from the resultant center of the steel beam compression zone to the neutral axis, A_{sc} is the sectional area of the steel beam compression zone, A_{st} is the sectional area of the steel beam tension zone, σ_d is the compressive strength of the straw board, A_d is the conversion area of the straw board, h_d is the thickness of the straw board. According to Eqs. (5), the flexural capacity of the normal section of the specimens FL-1~FL-3 are calculated as shown in Table 7.

Tab. 7 - Flexural capacities of composite slabs

Specimen No.	M_t/mm	M_c/mm	M_c/M_t
FL-1	11.09	11.39	1.03
FL-2	9.94	10.06	1.01
FL-3	10.23	10.01	0.98

M_c is the theoretical calculation value and M_t is the test value. It is found that the error between the theoretical deflection value and the test value is within 3% suggesting that Eqs. (5) can be used to calculate the flexural capacity of the composite slab.

CONCLUSIONS

(1) The tendency of lateral torsion buckling appeared, but the ultimate failure mode was local buckling of the steel beam, which indicated the straw board restrains the lateral torsion buckling of the lower steel beams.

(2) The composite action of the cold-formed thin-walled C-shaped steel-paper straw board composite slab is considerable, the straw board and the steel beam can deform coordinatively and fully exert the compressive performance of the straw board. Furthermore, the composite slab has high flexural capacity and meets the deflection limit of lightweight slab under the serviceability limit state, so it could be used in construction.

DOI 10.14311/CEJ.2020.01.0002

(3) Reducing the screw spacing between straw board and steel beam can significantly increase the yield load of composite slab, so the screw spacing should be moderately reduced to improve the flexural capacity of composite slab.

(4) Compared with other types of lightweight composite slabs, the cold-formed thin-walled C-shaped steel-paper straw board composite slab is of fine performance in deformation and flexural capacity, which can be able to meet the requirements of lightweight slab design.

(5) In the normal service stage, the equation is used to calculate the midspan deflection and the experimental value error of the composite slab within a reasonable range. The steel beams yield when the failure of the composite slab occur, the strain values of the straw board and the steel beam are basically the same, and the test values of the flexural capacity of composite slab agree well with that of the theoretical value. The equation for calculating the deflection and flexural capacity of composite slabs proposed is feasible.

ACKNOWLEDGEMENTS

This research is financially supported by the National Natural Science Foundation of China (51878130) and the Harbin Science and Technology Innovation Talent Research Special Foundation of China (2015RQQXJ078).

REFERENCES

[1] Garas G., Allam M., Dessuky El.R , 2009. Straw bale construction as an economic environmental building alternative - a case study. ARPN Journal of Engineering and Applied Sciences, Vol. 4, No. 9: 54-59.
[2] Taha Ashour , 2011. Performance of straw bale wall: a case of study.Energy and Buildings, Vol. 43: 1960-1967.
[3] Yin X.Z., Mike L., Daniel M., 2018. Construction and monitoring of experimental straw bale building in northeast China. Construction and Building Materials, Vol. 183: 46-57.
[4] Wright H.D., Evans H.R., Burt C.A., 1989. Profiled steel sheeting dryBoard composite slabs. The Structural Engineer, Vol. 67, No. 7: 114-129.
[5] Li Y.S., Shan W., Huang Z.B., 2008. Experimental study on mechanical behavior of profiled steel sheet-bamboo plywood composite slabs. Journal of Building Structures, Vol. 29, No.1: 96-102+111.
[6] Rahmadi A.P., Badaruzzaman W.H.W., Arifin A.K., 2013. Prediction of deflection of the composite profiled steel sheet MDF-board (PSSMDFB) slab system. Procedia Engineering, Vol. 54: 457-464.
[7] Zhou X.H., Li Z., Wang R.C., 2013. Study on load-carrying capacity of the cold-formed steel joists-OSB composite slab. China Civil Engineering Journal, Vol. 46, No. 9: 1-11.
[8] Shi Y., Zhou X.H., Song K., 2015. Study on flexural stiffness of cold-formed thin-walled steel joists-OSB composite slabs. Journal of Architecture and Civil Engineering, Vol. 32, No. 6: 50-57.
[9] Shan W., Li Y.S., Zhang X.H., 2016. Study on flexural behavior of cold-formed thin-walled C-shaped steel-bamboo rubber composite slab slab. Industrial Construction, Vol. 46, No. 1: 30-35.
[10] Kyvelou P., Gardner L., Nethercot D.A., 2017. Design of cold-formed steel composite slabing systems with partial shear connection. Ce/papers, Vol. 1, No. 2-3: 1899-1908.
[11] Jaeho R., Yong Yeal K., 2018. Experimental and numerical investigations of steel-polymer hybrid slab panels subjected to three-point flexural. Engineering Structures, Vol. 175: 467-482.
[12] Zhang X.H., Zhang Y.Z., Jun P., 2018. Experimental study on mechanical behavior of profiled steel sheet-strawboard composite slabs. Journal of Building Materials, Vol. 21, No. 6: 943-949.
[13] Kyvelou P., Gardner L., Nethercot D.A., 2018. Finite element modelling of composite cold-formed steel slabing systems. Engineering Structures, Vol. 158: 28-42.
[14] Zhou X.H., Shi Y., 2019. A simplified method to evaluate the flexural capacity of lightweight cold-formed steel slab system with oriented strand board subslab. Thin-Walled Structures, Vol. 134: 40-51.

[15] Kraus, Cynthia A., 1997. Slab vibration design criterion for cold-formed C-shaped supported residential slab systems. Blacksburg: Virginia Polytechnic Institute and State University.
[16] JGJ 227-2011, 2011. Technical specifications for low-rise cold-formed thin-walled steel buildings. China Building Industry Press.
[17] GB/T 228.1-2010, 2011. Metallic materials tensile testing part I: method of test at room temperature. China Standards Press.
[18] GB/T 31264-2014, 2015.Test methods for mechanical properties of structural wood-based panels. China Standard Press.